G. Oberti, L. Goffi, P.P. Rossi

Study of stratified rock masses by means of large-scale tests with a hydraulic pressure chamber

(paper presented at the *V International Congress on Rock Mechanics,* Melbourne, april 10-15, 1983)

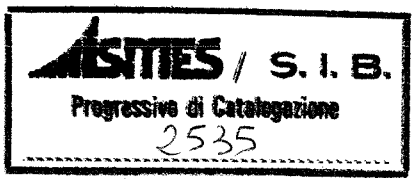

istituto sperimentale modelli e strutture s.p.a. viale Giulio Cesare, 29 - 24100 BERGAMO - tel. 243043 - telex 301249 - BG

STUDY OF STRATIFIED ROCK MASSES BY MEANS OF LARGE-SCALE TESTS WITH AN HYDRAULIC PRESSURE CHAMBER

Etudes d'amas rocheux stratifiés par essais in-situ avec chambre à pression hydraulique

Untersuchung geschichteter felsiger Anhäufungen mit in-situ Druckkammerversuchen

G. Oberti
Prof.Ing., ISMES President, Bergamo, Italy

L. Goffi
Prof.Ing., Polytechnic of Turin, Italy

P. P. Rossi
Dr.Ing., ISMES Geomechanical Dept., Bergamo, Italy

SYNOPSIS

This paper discusses the identification of elastic constants of stratified rock through large-scale in-situ tests with an hydraulic pressure chamber. Above all the anisotropy parameteres of a stratified mass have been stated as a function of moduli and thicknesses of the layers. The influence of the stratification is analysed with reference to the equivalent crystalline anisotropy. Experimental measures performed by a special technique in a stratified rock mass consisting of alternating layers of sandstone and marl have been analysed and interpreted in comparison with the results of the theoretical approach. Finally the most recent development of ISMES testing technique is illustrated and discussed.

RESUME

Dans ce rapport on examine le problème de la détermination des constantes élastiques de roches stratifiées au moyen d'essais in-situ à grande échelle avec chambre à pression hydraulique. On rappelle d'abord tous les paramètres d'anisotropie qui caractérisent un amas rocheux stratifié en fonction des modules élastiques et des épaisseurs de couches. L'influence de la stratification est analysée par rapport à l'anisotropie cristalline équivalente. Ensuite on analyse les résultats de mesures effectuées avec instrumentation spéciale dans un amas rocheux stratifié constitué de grès et marne. Les données expérimentales sont comparées aux résultats fournis par le calcul théorique. Enfin, on illustre et discute les plus récents développements de la technique d'essais avec chambre hydraulique mise au point par ISMES.

ZUSAMMENFASSUNG

Berichtet wird über die Untersuchung des Problems der Bestimmung der eleastischen Konstanten geschichteten Felsens durch großmaßstäbliche in-situ Versuche mit einer hydraulischen Druckkammer. Vor allem werden die Anisotropie-Parameter aufgeführt, die geschichteten Fels in Abhängigkeit der elastischen Moduln und der Schichtmächtigkeit charakterisieren. Der Einfluß der Schichtung wird unter Bezug auf die äquivalente kristalline Anisotropie analysiert. Die Meßergebnisse werden fernerhin mit Hilfe einer Spezial-Instrumentierung in einem aus Sandstein und Mergel bestehenden Gebirge überprüft. Die Versuchsergebnisse werden an Hand der sich durch theoretische Berechnung erhaltenen Ergebnisse überprüft. Abschließend werden die neuesten Entwicklungen der von ISMES ausgearbeiteten Versuchstechnik mit einer hydraulischen Druckkammer erläutert.

1. "CRYSTALLINE" ANISOTROPY

The stress-strain relationships for anisotropic elastic continua are recalled:

$$|\varepsilon| = |K| \cdot |\sigma| \qquad (1)$$

or

$$\varepsilon_x = \frac{\sigma_x}{E_1} - \frac{\nu_2}{E_2}\sigma_y - \frac{\nu_1}{E_1}\sigma_z$$

$$\varepsilon_y = -\frac{\nu_2}{E_2}\sigma_x + \frac{\sigma_y}{E_2} - \frac{\nu_2}{E_2}\sigma_z$$

$$\varepsilon_z = -\frac{\nu_1}{E_1}\sigma_x - \frac{\nu_2}{E_2}\sigma_y + \frac{\sigma_z}{E_1}$$

$$\gamma_{xz} = \frac{2(1+\nu_1)}{E_1}\tau_{xz}$$

$$\gamma_{xy} = \frac{\tau_{xy}}{G_2} \qquad \gamma_{yz} = \frac{\tau_{yz}}{G_2}$$

Applying equilibrium and compatibility relationships, and considering problems of plane elasticity (on the plane x, y) in the case of confined transversal strains $\sigma_z = 0$, if we assume

$$\sigma_x = \frac{\partial^2 \phi}{\partial y^2} \qquad \sigma_y = \frac{\partial^2 \phi}{\partial x^2} \qquad \tau_{xy} = -\frac{\partial^2 \phi}{\partial x \partial y}$$

we obtain:

$$\frac{1-\nu_1^2}{E_1}\frac{\partial^4\phi}{\partial y^4}+\left[\frac{1}{G_2}-\frac{2\nu_2(1+\nu_1)}{E_2}\right]\frac{\partial^4\phi}{\partial x^2\partial y^2}+\left[\frac{1-n\nu_2^2}{E_2}\right]\frac{\partial^4\phi}{\partial x^4}=0 \quad (2)$$

The problem discussed is that of a circular tunnel of radius R in a indefinite mass of orthotropic elastic rock. The tunnel axis is made to coincide with axis z (Fig. 1). The tunnel is subjected to uniform pressure

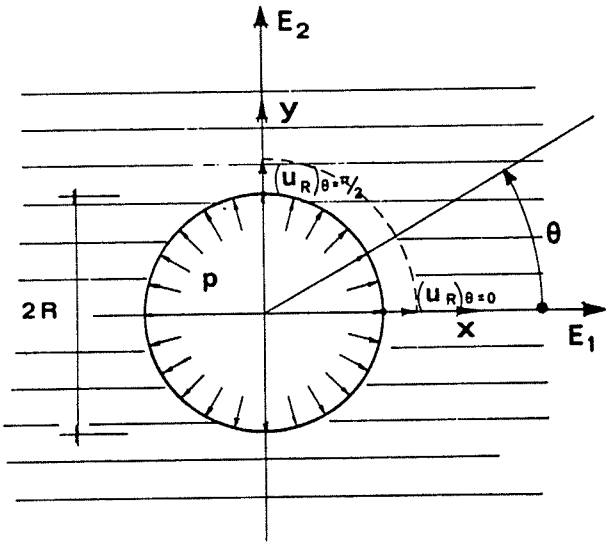

FIG. 1 Scheme of hydraulic pressure chamber test.

p. We propose the calculation of radial displacements at each point of the continuum, but in particular of the points on axes x and y, that is for $\vartheta = 0$ and $\vartheta = \pi/2$ (see Fig. 1).

The solution of the (2), from which values of radial displacement may be derived, exists in a concluded form, however it is remarkably complicated. It has therefore been preferred resorting to a numerical solution. Simple formulae may, on the other hand, be written for displacements of points at the tunnel edge, that is for r = = R

$$(u_R)_{\theta=0}=\frac{pR}{E_1}\left\{(1-\nu_1^2)\left[\sqrt{\frac{1}{1-\nu_1^2}\left[\frac{n}{m}-2n\nu_2(1+\nu_1)\right]}+2\sqrt{n}\sqrt{\frac{1-n\nu_2^2}{1-\nu_1^2}}-\right.\right.$$

$$\left.\left.-\sqrt{n}\sqrt{\frac{1-n\nu_2^2}{1-\nu_1^2}}\right]+n\nu_2(1+\nu_1)\right\} \quad (3)$$

$$(u_R)_{\theta=\pi/2}=\frac{pR}{E_1}\left\{\sqrt{n}\cdot\sqrt{1-n\nu_2^2}\cdot\sqrt{1-\nu_1^2}\cdot\right.$$

$$\left.\cdot\left[\sqrt{\frac{1}{1-\nu_1^2}\left[\frac{n}{m}-2n\nu_2(1+\nu_1)\right]}+2\sqrt{n}\sqrt{\frac{1-n\nu_2^2}{1-\nu_1^2}}-1\right]+n\nu_2(1+\nu_1)\right\}$$

where it was assumed

$$n = E_1/E_2 \qquad m = G_2/E_2 .$$

Values of u_R have been calculated and indicated in Table I and diagram of Fig. 2 (in the dimensionless form $\frac{u_R}{(p\,R)/E_1}$ versus n and m).

TABLE I

n	m	$\frac{(u_R)\,\theta=0}{p\,R/E_1}$	$\frac{(u_R)\,\theta=\pi/2}{p\,R/E_1}$
1	0.2	1.766	1.766
	0.4	1.224	1.224
	0.6	1.006	1.006
2	0.2	2.502	3.790
	0.4	1.686	2.661
	0.6	1.348	2.193
3	0.2	3.137	5.776
	0.4	2.106	4.068
	0.6	1.672	3.347
4	0.2	3.724	7.697
	0.4	2.511	5.426
	0.6	1.993	4.456

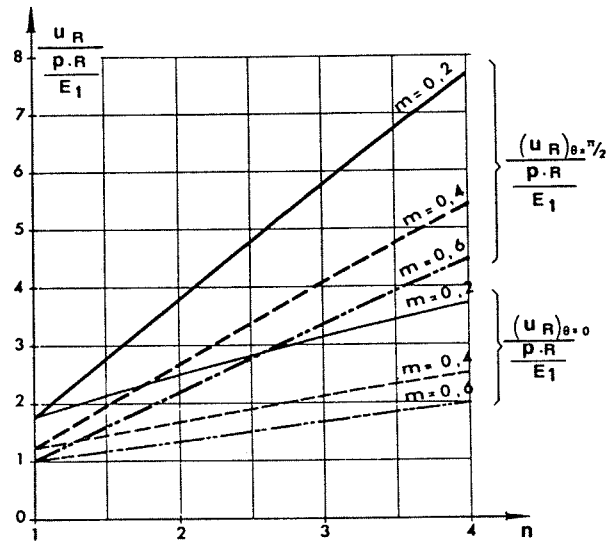

FIG. 2 Radial displacements along principal axes as a function of $n = E_1/E_2$.

The values of the displacements inside the rock mass obtained from the numerical solution of the (2) are reported in Table II still in dimensionless form. ν_1 and ν_2 were assumed equal to 0.2. Values of G_2 were supposed such as to give rise to the following ratios:

$$m = \frac{G_2}{E_2} = 0.2 - 0.4 - 0.6$$

In Fig. 3, the ratio of radial displacement u_r (at a distance r from the tunnel center) to the displacement at the tunnel edge u_R, is plotted versus r/R, using m and n as parameters.

TABLE II

$\frac{u_R}{p \cdot R/E_1}$

$n = \frac{E_1}{E_2}$	$m = \frac{G_2}{E_2}$	θ = 0				θ = π/2			
		R	2R	3R	5R	R	2R	3R	5R
4	0.2	3.6266	2.5399	2.0133	1.4066	7.6266	4.9466	3.6199	2.3066
	0.4	2.4266	1.4453	1.0506	0.6733	5.3733	3.0279	2.0906	1.2799
	0.6	1.9199	0.9999	0.6799	0.4133	4.4133	2.2599	1.5186	0.9133
2.6666	0.2	2.8799	1.9599	1.5119	1.0199	5.0799	3.2466	2.3613	1.4999
	0.4	1.9199	1.0999	0.7786	0.4866	3.5733	1.9693	1.3506	0.8199
	0.6	1.5199	0.7599	0.5039	0.2999	2.9466	1.4666	0.9786	0.5886
2	0.2	2.4799	2.6399	1.2426	0.8133	3.7599	2.3799	1.7226	1.0933
	0.25	2.1733	1.3706	1.0093	0.6466	3.3466	2.0266	1.4399	0.8933
	0.30	1.9599	1.1813	0.8506	0.5399	2.9733	1.7199	1.2039	0.7599
	0.40	1.6666	0.9253	0.6426	0.3933	2.6399	1.4293	0.9746	0.5933
1.5384	0.4153	1.4399	0.7639	0.5213	0.3133	1.9466	1.0226	0.6926	0.4199
1.3333	0.2	2.0266	1.2799	0.9413	0.5999	2.4399	1.5133	1.0916	0.6866
	0.4	1.3733	0.7266	0.4906	0.2999	1.6933	0.8866	0.5986	0.3666
1	0.2	1.7599	1.0799	0.7693	0.4866	1.7599	1.0799	0.7706	0.4866
	0.4	1.2239	0.6199	0.4146	0.2466	1.2253	0.6199	0.4146	0.2466
	0.415	1.1999	0.5999	0.3986	0.2399	1.1999	0.5999	0.3896	0.2399

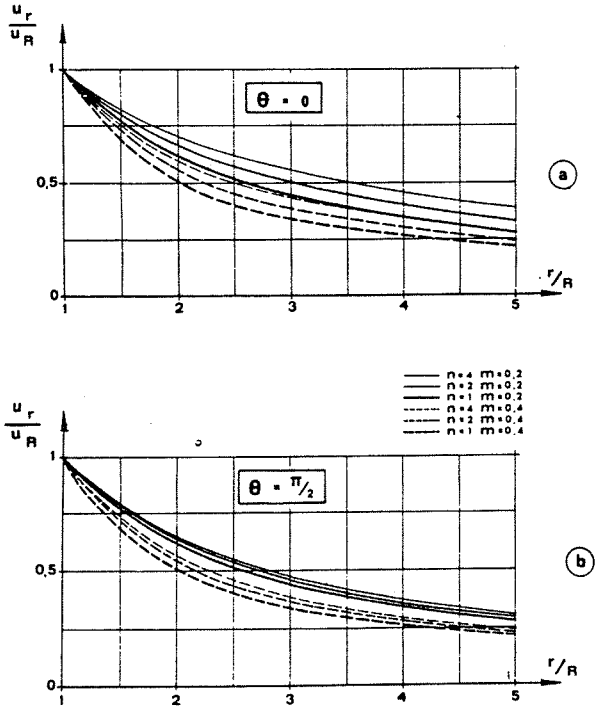

FIG. 3 Ratios between internal and surface radial displacement.

2. "STRATIFIED" ANISOTROPY

Previous conclusions may be applied to the case of stratified rock mass, the orthotropy of which results from a regular alternation of layers of two isotropic materials A and B of Young's moduli E_A and E_B, Poisson's ratios ν_A and ν_B and thicknesses s_A and s_B as deduced from a previous study (Borsetto et al., 1981). This study starts from Pinto's formulae (1966), which make it possible to calculate the orthotropy parameters resulting from the stratification in terms of E_1, E_2, G_2, ν_1 and ν_2 equivalent for a "crystalline homogeneous medium":

$$E_1=\frac{\left[(1+\nu_A)+(1+\nu_B)\frac{s_A}{s_B}\cdot\frac{E_A}{E_B}\right]\left[(1-\nu_A)+(1-\nu_B)\frac{s_A}{s_B}\frac{E_A}{E_B}\right]\cdot E_A}{\left[(1-\nu_A^2)+(1-\nu_B^2)\frac{s_A}{s_B}\cdot\frac{E_A}{E_B}\right]\left(1+\frac{s_A}{s_B}\right)\cdot\frac{E_A}{E_B}}$$

$$E_2=\frac{\left[(1-\nu_A)+(1-\nu_B)\frac{s_A}{s_B}\cdot\frac{E_A}{E_B}\right]\left(1+\frac{s_A}{s_B}\right)\cdot E_A}{\left[(1-\nu_A)+(1-\nu_B)\frac{s_A}{s_B}\cdot\frac{E_A}{E_B}\right]\left(\frac{s_A}{s_B}+\frac{E_A}{E_B}\right)-2\left(\nu_A-\nu_B\frac{E_A}{E_B}\right)^2\cdot\frac{s_A}{s_B}}$$

$$G_2=\frac{1+\frac{s_A}{s_B}}{2\left[(1+\nu_A)\frac{s_A}{s_B}+(1+\nu_B)\frac{E_A}{E_B}\right]}\cdot E_A \qquad (4)$$

$$\nu_1=\frac{(1-\nu_A^2)\nu_B+(1-\nu_B^2)\frac{s_A}{s_B}\cdot\frac{E_A}{E_B}\nu_A}{(1-\nu_A^2)+(1-\nu_B^2)\cdot\frac{s_A}{s_B}\cdot\frac{E_A}{E_B}}$$

$$\nu_2=\frac{\left[(1-\nu_A)\nu_B+(1-\nu_B)\frac{s_A}{s_B}\cdot\nu_A\right]\left(1+\frac{s_A}{s_B}\right)\frac{E_A}{E_B}}{\left[(1-\nu_A)+(1-\nu_B)\frac{s_A}{s_B}\cdot\frac{E_A}{E_B}\right]\left(\frac{s_A}{s_B}+\frac{E_A}{E_B}\right)-2\left(\nu_A-\frac{E_A}{E_B}\cdot\nu_B\right)^2\frac{s_A}{s_B}}$$

If then we assume

$$a=\frac{s_A}{s_B} \qquad E=\frac{E_A}{E_B}$$

and $\nu_A=\nu_B=\nu$,

the aforesaid expressions are simplified in the form

$$E_1 = \frac{1 + a\,e}{(1+a)\cdot e}\,E_A$$

$$E_2 = \frac{(1+a\,e)(1+a)}{(1+a\,e)(a+e) - 2\nu^2\,\frac{(1-e)^2 a}{1-\nu}}\,E_A$$

$$G_2 = \frac{1+a}{2\,(1+\nu)\,(a+e)}\,E_A$$

$$\nu_1 = \nu$$

$$\nu_2 = \frac{(1+a)^2\,\nu\cdot e}{(1+a\,e)(a+e) - \frac{2\nu^2}{1-\nu}\,(1-e)^2 a}$$

Ratios n and m result therefore from expressions:

$$n = \frac{(1+a\,e)(a+e) - \frac{2\nu^2}{1-\nu}\,(1-e)^2 a}{e\,(1+a)^2}$$

$$m = \frac{(a+e)(1+a\,e) - \frac{2\nu^2}{1-\nu}\,(1-e)^2 a}{2\,(1+\nu)(a+e)(1+a\,e)}$$

and are plotted together with ν_2 versus a and e, in Figs. 4, 5, 6 (*).

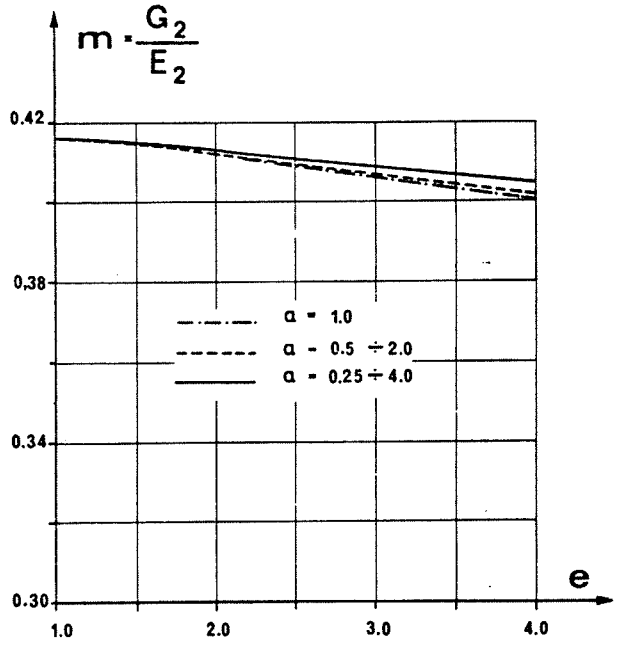

FIG. 5 Ratio between equivalent moduli G_2 and E_2 as a function of e and a.

(*) For semplicity's sake, $e \geq 1$ was assumed in the diagrams, that is $E_A \geq E_B$; curves for individual values of a are also valid for inverse values, that is for 1/a, given the form of expressions for n and m.

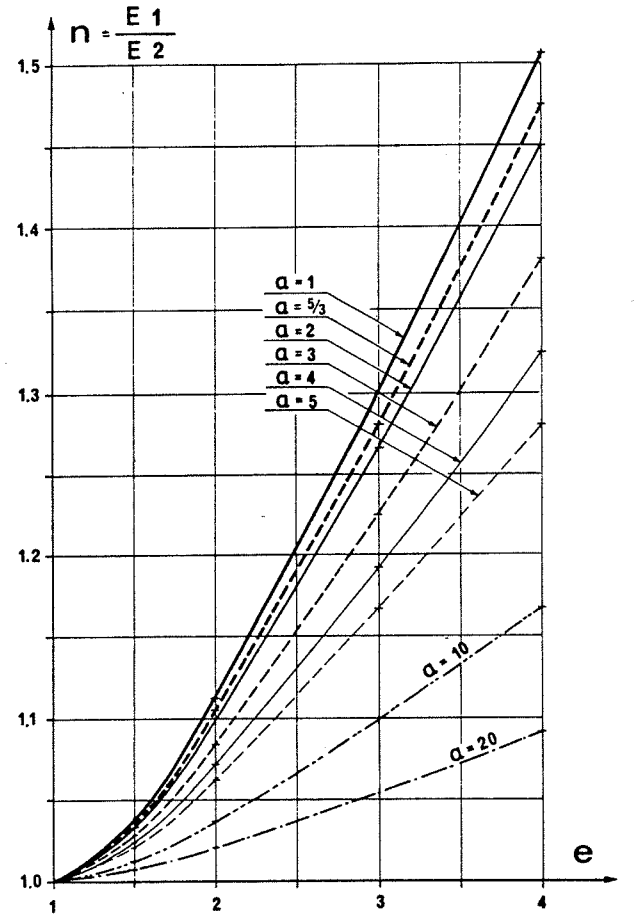

FIG. 4 Ratio of equivalent Young's moduli as a function of the ratios of component material moduli ($e = E_A/E_B$) and thicknesses ($a = s_A/s_B$).

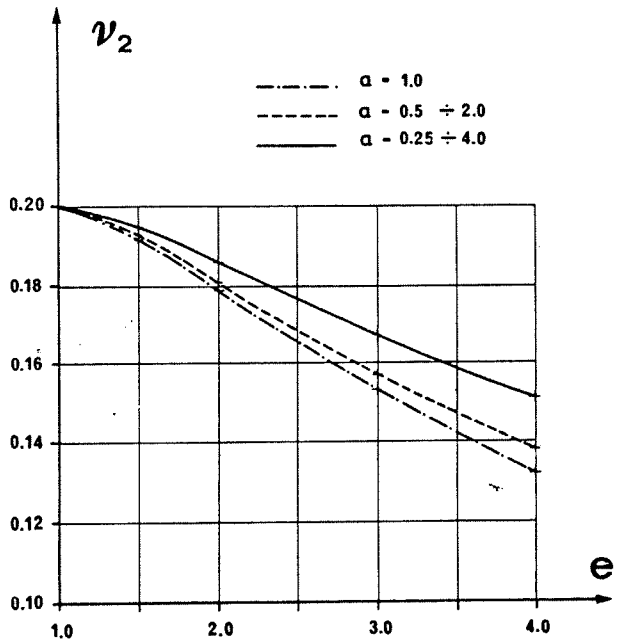

FIG. 6 Equivalent Poisson's ratio ν_2 as a function of e and a.

TABLE II

$\frac{u_R}{p \cdot R/E_1}$

$n = \frac{E_1}{E_2}$	$m = \frac{G_2}{E_2}$	θ = 0				θ = π/2			
		R	2R	3R	5R	R	2R	3R	5R
4	0.2	3.6266	2.5399	2.0133	1.4066	7.6266	4.9466	3.6199	2.3066
	0.4	2.4266	1.4453	1.0506	0.6733	5.3733	3.0279	2.0906	1.2799
	0.6	1.9199	0.9999	0.6799	0.4133	4.4133	2.2599	1.5186	0.9133
2.6666	0.2	2.8799	1.9599	1.5119	1.0199	5.0799	3.2466	2.3613	1.4999
	0.4	1.9199	1.0999	0.7786	0.4866	3.5733	1.9693	1.3506	0.8199
	0.6	1.5199	0.7599	0.5039	0.2999	2.9466	1.4666	0.9786	0.5886
2	0.2	2.4799	2.6399	1.2426	0.8133	3.7599	2.3799	1.7226	1.0933
	0.25	2.1733	1.3706	1.0093	0.6466	3.3466	2.0266	1.4399	0.8933
	0.30	1.9599	1.1813	0.8506	0.5399	2.9733	1.7199	1.2039	0.7599
	0.40	1.6666	0.9253	0.6426	0.3933	2.6399	1.4293	0.9746	0.5933
1.5384	0.4153	1.4399	0.7639	0.5213	0.3133	1.9466	1.0226	0.6926	0.4199
1.3333	0.2	2.0266	1.2799	0.9413	0.5999	2.4399	1.5133	1.0916	0.6866
	0.4	1.3733	0.7266	0.4906	0.2999	1.6933	0.8866	0.5986	0.3666
1	0.2	1.7599	1.0799	0.7693	0.4866	1.7599	1.0799	0.7706	0.4866
	0.4	1.2239	0.6199	0.4146	0.2466	1.2253	0.6199	0.4146	0.2466
	0.415	1.1999	0.5999	0.3986	0.2399	1.1999	0.5999	0.3896	0.2399

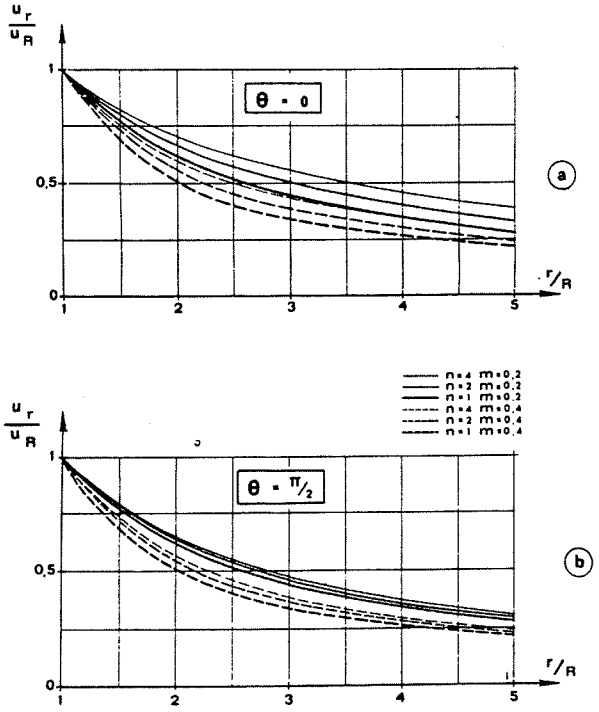

FIG. 3 Ratios between internal and surface radial displacement.

2. "STRATIFIED" ANISOTROPY

Previous conclusions may be applied to the case of stratified rock mass, the orthotropy of which results from a regular alternation of layers of two isotropic materials A and B of Young's moduli E_A and E_B, Poisson's ratios ν_A and ν_B and thicknesses s_A and s_B as deduced from a previous study (Borsetto et al., 1981). This study starts from Pinto's formulae (1966), which make it possible to calculate the orthotropy parameters resulting from the stratification in terms of E_1, E_2, G_2, ν_1 and ν_2 equivalent for a "crystalline homogeneous medium":

$$E_1 = \frac{\left[(1+\nu_A) + (1+\nu_B)\frac{s_A}{s_B}\cdot\frac{E_A}{E_B}\right]\left[(1-\nu_A) + (1-\nu_B)\frac{s_A}{s_B}\cdot\frac{E_A}{E_B}\right]\cdot E_A}{\left[(1-\nu_A^2) + (1-\nu_B^2)\frac{s_A}{s_B}\cdot\frac{E_A}{E_B}\right]\left(1+\frac{s_A}{s_B}\right)\cdot\frac{E_A}{E_B}}$$

$$E_2 = \frac{\left[(1-\nu_A) + (1-\nu_B)\frac{s_A}{s_B}\cdot\frac{E_A}{E_B}\right]\left(1+\frac{s_A}{s_B}\right)\cdot E_A}{\left[(1-\nu_A) + (1-\nu_B)\frac{s_A}{s_B}\cdot\frac{E_A}{E_B}\right]\left(\frac{s_A}{s_B}+\frac{E_A}{E_B}\right) - 2\left(\nu_A - \nu_B\frac{E_A}{E_B}\right)^2\cdot\frac{s_A}{s_B}}$$

$$G_2 = \frac{1+\frac{s_A}{s_B}}{2\left[(1+\nu_A)\frac{s_A}{s_B} + (1+\nu_B)\frac{E_A}{E_B}\right]}\cdot E_A \qquad (4)$$

$$\nu_1 = \frac{(1-\nu_A^2)\nu_B + (1-\nu_B^2)\frac{s_A}{s_B}\cdot\frac{E_A}{E_B}\nu_A}{(1-\nu_A^2) + (1-\nu_B^2)\cdot\frac{s_A}{s_B}\cdot\frac{E_A}{E_B}}$$

$$\nu_2 = \frac{\left[(1-\nu_A)\nu_B + (1-\nu_B)\frac{s_A}{s_B}\cdot\nu_A\right]\left(1+\frac{s_A}{s_B}\right)\frac{E_A}{E_B}}{\left[(1-\nu_A) + (1-\nu_B)\frac{s_A}{s_B}\cdot\frac{E_A}{E_B}\right]\left(\frac{s_A}{s_B}+\frac{E_A}{E_B}\right) - 2\left(\nu_A - \frac{E_A}{E_B}\cdot\nu_B\right)^2\frac{s_A}{s_B}}$$

If then we assume

$$a = \frac{s_A}{s_B} \qquad E = \frac{E_A}{E_B}$$

and $\nu_A = \nu_B = \nu$,

the aforesaid expressions are simplified in the form

$$E_1 = \frac{1 + a\,e}{(1+a)\cdot e}\,E_A$$

$$E_2 = \frac{(1+a\,e)(1+a)}{(1+ae)(a+e) - 2\nu^2\,\frac{(1-e)^2 a}{1-\nu}}\,E_A$$

$$G_2 = \frac{1+a}{2\,(1+\nu)\,(a+e)}\,E_A$$

$$\nu_1 = \nu$$

$$\nu_2 = \frac{(1+a)^2\,\nu\cdot e}{(1+ae)(a+e) - \frac{2\nu^2}{1-\nu}\,(1-e)^2\cdot a}$$

Ratios n and m result therefore from expressions:

$$n = \frac{(1+ae)(a+e) - \frac{2\nu^2}{1-\nu}\,(1-e)^2 a}{e\,(1+a)^2}$$

$$m = \frac{(a+e)(1+ae) - \frac{2\nu^2}{1-\nu}\,(1-e)^2 a}{2\,(1+\nu)(a+e)(1+ae)}$$

and are plotted together with ν_2 versus a and e, in Figs. 4, 5, 6 (*).

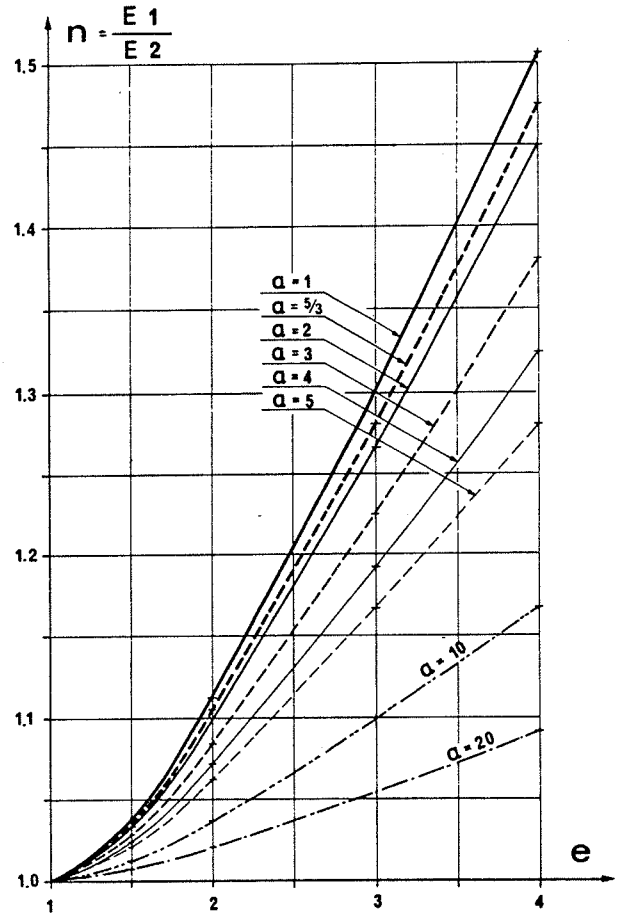

FIG. 4 Ratio of equivalent Young's moduli as a function of the ratios of component material moduli (e= = E_A/E_B) and thicknesses (a= s_A/s_B).

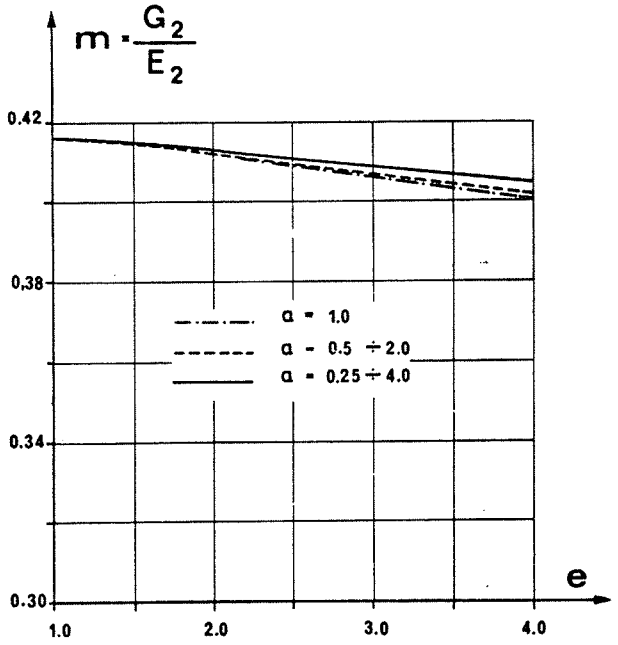

FIG. 5 Ratio between equivalent moduli G_2 and E_2 as a function of e and a.

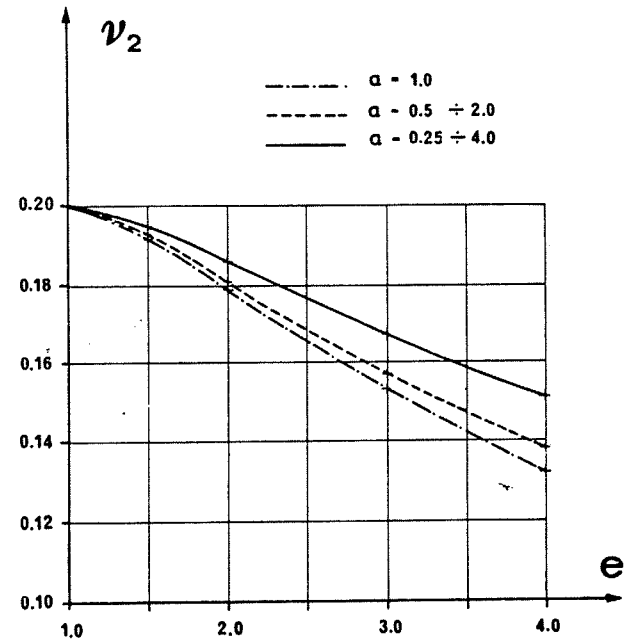

FIG. 6 Equivalent Poisson's ratio ν_2 as a function of e and a.

(*) For semplicity's sake, $e \geq 1$ was assumed in the diagrams, that is $E_A \geq E_B$; curves for individual values of a are also valid for inverse values, that is for 1/a, given the form of expressions for n and m.

As already pointed out, also with high values of the ratio e between moduli E_A and E_B of stratification materials (up to 4) we do not succeed in obtaining, for the ratio n (between equivalent Young's moduli E_1 and E_2) values higher than 1.5. Moreover, the orthotropy deriving from stratification of isotropic materials actually supposes a link between G_2 and E_2. Indeed, as it also clearly appears from the diagram of Fig. 5, $m = G_2/E_2$ is slightly affected by $a = s_A/s_B$ and $e = E_A/E_B$, practically ranging from 0.40 to 0.416. This property also results from the analysis of the formula m which may be written

$$m = \frac{1}{2(1+\nu)} - \frac{\nu^2 (1-e)^2 a}{(1-\nu^2)(a+e)(1+ae)}$$

where the second term is negligible compared with the first one. Therefore G_2 would simply be expressed by

$$G_2 \cong \frac{E_2}{2(1+\nu)}$$

which has the same form of the relationship between G and E for isotropic continua.

The link between G_2 and E_2 may allow to obtain the elastic constants from the simple measure of radial displacements for $\vartheta = 0$ and $\vartheta = \pi/2$, without supplementary tests. The three principal unknows E_1, E_2 and G_2 are derived from these two measurements, as the third equation is obtained from the aforesaid: $G_2 \cong E_2/[2(1+\nu)]$.

3. SOME EXAMPLES OF F.E.M. CALCULATIONS ON STRATIFIED MEDIA

A study on the actual stratification influence had been undertaken (Borsetto et al., 1981) for a wide case history summarized in Fig. 7. The two cases $e = E_A/E_B = 2$ and 4 had moreover been assumed. Then diametral displacements due to water pressure were calculated for $\vartheta = 0$ and $\vartheta = \pi/2$; the results were compared with those consequent to the assumption of equivalent "crystalline" orthotropy. Results are shown in Table III, and in diagram of Fig. 8. In particular, Fig. 8 shows in abscissa the values of radial displacements, computed in the various assumptions of stratifications, and in ordinate the corresponding values consequent from the assumption of "crystalline" anisotropy. The thickening of points close to a straight line at 45° shows the good correlation between the two assumptions, at least in the 9 cases considered. Therefore we may consider correct the interpretation of experimental results in hydraulic chamber in stratified masses by "crystalline" orthotropy formulae, which therefore may give the equivalent Young's moduli of the rock mass.

4. AN EXAMPLE OF INTERPRETATION OF EXPERIMENTAL RESULTS OBTAINED BY HYDRAULIC PRESSURE CHAMBER

The formulae discussed in the previous sections were applied to the processing of the results of tests carried out at the foundation rock of Ridracoli Dam, located in the province of Forlì. The dam is an arch-gravity structure, max height 120 m, crest length about 400 m; it closes off the River Bidente, forming a reservoir of about 35 million m^3 capacity.

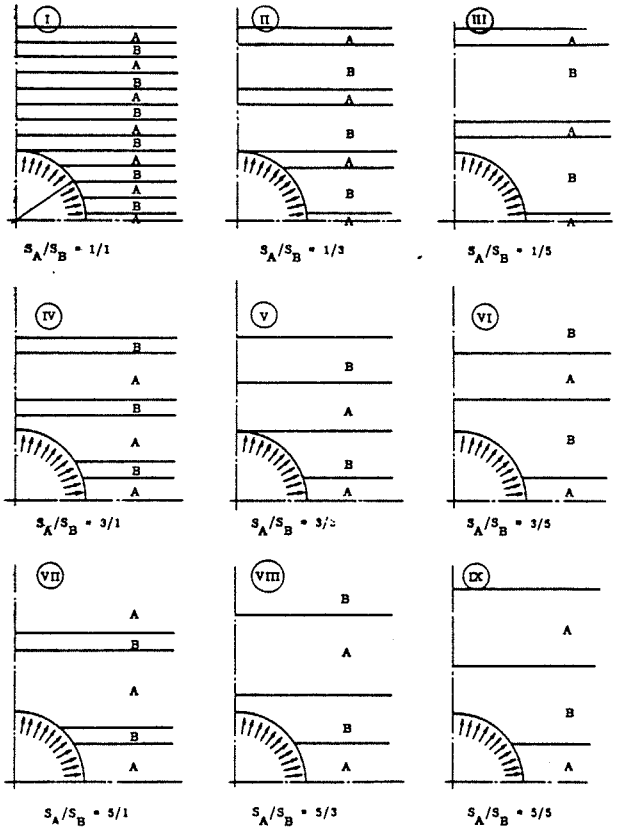

FIG. 7 Alternating schemes of stratifications concerned with displacement computation by F.E.M.

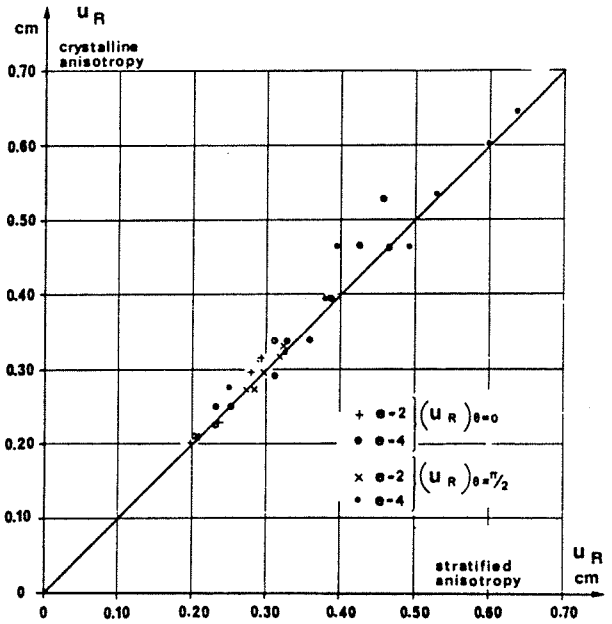

FIG. 8 Comparison between radial displacements in the assumption of crystalline and stratified anisotropy.

TABLE III (*)

								Hydraulic chamber stratified anisotropy		Hydraulic chamber crystalline anisotropy	
Scheme	S_A	S_B	$a = \frac{S_A}{S_B}$	$e = \frac{E_A}{E_B}$	E_1 / Kg cm^{-2}	E_2 / Kg cm^{-2}	n	$(u_R)_{\theta=0}$ / cm	$(u_R)_{\theta=\pi/2}$ / cm	$(u_R)_{\theta=0}$ / cm	$(u_R)_{\theta=\pi/2}$ / cm
I	1	1	1	2	75000	67615	1.1125	0.245	0.273	0.250	0.274
				4	62500	41493	1.506	0.392	0.463	0.3384	0.4644
II	1	3	1/3	2	62499	57636	1.0843	0.280	0.318	0.297	0.3174
				4	43749	31709	1.3791	0.425	0.592	0.4663	0.6021
III	1	5	1/5	2	58333	54901	1.0625	0.293	0.326	0.3159	0.3320
				4	37500	29268	1.2812	0.457	0.617	0.5825	0.665
IV	3	1	3	2	87500	80691	1.08438	0.204	0.229	0.2121	0.2267
				4	81250	58900	1.3795	0.235	0.326	0.2510	0.3241
V	3	3	1	2	75000	67415	1.1125	0.236	0.254	0.250	0.2760
				4	62500	41493	1.506	0.312	0.395	0.3384	0.4666
VI	3	5	3/5	2	68750	62190	1.1056	0.256	0.297	0.2117	0.2952
				4	53125	36026	1.4746	0.386	0.529	0.3951	0.5352
VII	5	1	5	2	91666	86274	1.0625	0.198	0.205	0.2010	0.2113
				4	87500	68292	1.2812	0.226	0.251	0.2265	0.2164
VIII	5	3	5/3	2	81249	73498	1.1056	0.235	0.249	0.2299	0.2498
				4	71874	48741	1.47461	0.312	0.382	0.2920	0.3955
IX	5	5	1	2	75000	67415	1.1125	0.252	0.285	0.250	0.2740
				4	62500	41493	1.506	0.359	0.493	0.3384	0.4644

(*) The values have been calculated following these assumptions: Radius R = 150 cm, Young modulus of material A: E_A = 100,000 Kg cm^{-2}, inner hydraulic pressure p_o = 100,000 Kg cm^{-2}.

The foundation rock mass consists of alternating sandstone and marl, with layers diping about 28° (Fig. 9).

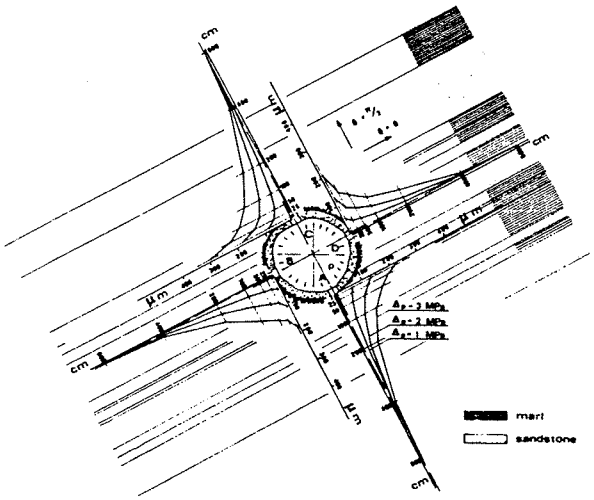

FIG. 9 Hydraulic chamber test on the stratified rock mass at the Ridracoli Dam. Diagrams of radial displacement as a function of depth for 3 levels of internal pressure.

Since layers are 100 to 150 cm thick, large-scale tests were carried out to determine deformability characteristics, using the hydraulic pressure chamber technique. Tests were performed inside two 3 m-diam tunnels, their axis being parallel to stratification planes on the two banks of the dam, at its foundation. The procedures of the tests are described in paragraph 5.

In the comparison of the theoretical and experimental data, we consider, for statical purposes, the radius of the tunnel equal to 157 cm, 7 cm being the depth of the point related to the most superficial measure. In fact we have measured the radial displacements (along the axes perpendicular and parallel to the stratification plane) at different depths as relative to a reference point located at 750 cm from the center of the tunnel (at a depth of two times the diameter of the chamber).

The radial displacements have been measured at the distances of 157 - 175 - 200 - 250 - 350 - 550 cm from the center of the tunnel; the values are the reversible displacements at three different levels of inner pressure (1 - 2 - 3 MPa) starting from a ground pressure of 1.2 MPa (Table IV and Fig. 9). These pressures are relative to the 150 cm radius; therefore, if referred to the "static" radius of 157 cm, the pressures become, according to $\Delta p' = (150/157)\,\Delta p$, 0.955 - 1.911 - 2.866 MPa.

The theoretical and experimental values of the radial displacements have been elaborated considering that the effective radius of the tunnel is 157 cm and the reference point of the displacements is located at 750 cm from the center of the tunnel (Tables V and VI). Experimental values (**) are plotted in Figs. 10 and

(**) From average values of the two opposite measurements (A+C)/2 and (B+D)/2 according to Table IV and Fig.9.

TABLE IV

Reversible radial displacements (μm) at the points A,B,C,D (see Fig.9)

Ground pressure 1.2 MPa

Δp (MPa)	depth d (cm)	A	B	C	D
3	7	220	188	295	208
	25	182	149	214	138
	50	146	138	166	115
	100	101	112	120	79
	200	52	61	70	53
	400	7	10	11	10
2	7	129	112	176	125
	25	107	88	125	83
	50	84	81	94	68
	100	56	63	67	48
	200	26	34	36	25
	400	2	5	5	5
1	7	59	48	84	51
	25	50	37	55	35
	50	39	34	38	29
	100	25	26	25	21
	200	12	13	12	10
	400	2	0	0	0

TABLE V $\vartheta = 0$

$n = \frac{E_1}{E_2}$	$m = \frac{G_2}{E_2}$	$\frac{u_r - u_{750}}{p \frac{R}{E_1}}$			$\frac{u_r - u_{750}}{u_{R'} - u_{750}}$		
		R'	2R'	3R'	R'	2R'	3R'
4	0.2	2.1541	1.0674	0.5408	1	0.4955	0.2510
	0.4	1.7121	0.7308	0.3361	1	0.4269	0.1963
	0.6	1.4775	0.5575	0.2375	1	0.3773	0.1607
2.6666	0.2	1.8065	0.8865	0.4385	1	0.4907	0.2427
	0.4	1.4014	0.5814	0.2601	1	0.4149	0.1856
	0.6	1.1977	0.4377	0.1817	1	0.3655	0.1517
2	0.2	1.6198	0.7798	0.3825	1	0.4814	0.2361
	0.25	1.4871	0.6844	0.3231	1	0.4602	0.2173
	0.3	1.2861	0.6075	0.2768	1	0.4383	0.1997
	0.4	1.2461	0.5048	0.2221	1	0.4051	0.1782
1.5384	0.4153	1.1039	0.4279	0.1853	1	0.3876	0.1679
1.3333	0.2	1.2895	0.6428	0.3042	1	0.4626	0.2189
	0.4	1.0526	0.4059	0.1699	1	0.3856	0.1614
1	0.2	1.2425	0.5625	0.2519	1	0.4527	0.2027
	0.4	0.9589	0.3549	0.1496	1	0.3701	0.1560
	0.415	0.9427	0.3427	0.1414	1	0.3635	0.1500

11 versus the distance from the tunnel edge as ratios to the relative deformations measured at 7 cm depth; on these diagrams have been plotted also the corresponding theoretical curves for the case of the isotropy and anisotropy (n = 4, m = 0.4).

A good agreement can be observed between the decreasing of experimental and theoretical values of the above ratios. This fact confirms the reliability of the experimental results.

TABLE VI $\vartheta = \pi/2$

$n = \frac{E_1}{E_2}$	$m = \frac{G_2}{E_2}$	$\frac{u_r - u_{750}}{\Delta p \frac{R}{E_1}}$			$\frac{u_r - u_{750}}{u_{R'} - u_{750}}$		
		R'	2R'	3R'	R'	2R'	3R'
4	0.2	5.1766	2.4966	1.1699	1	0.4823	0.2260
	0.4	4.0047	1.6593	0.7220	1	0.4144	0.1803
	0.6	3.4338	1.2804	0.5391	1	0.3729	0.1570
2.6666	0.2	3.4859	1.6526	0.7673	1	0.4741	0.2201
	0.4	2.6959	1.0919	0.4732	1	0.4050	0.1755
	0.6	2.3171	0.8371	0.3491	1	0.3613	0.1507
2	0.2	2.5979	1.2179	0.5606	1	0.4688	0.2158
	0.25	2.3936	1.0736	0.4869	1	0.4485	0.2034
	0.3	2.1649	0.9115	0.3955	1	0.4211	0.1827
	0.4	2.0049	0.7943	0.3396	1	0.3962	0.1694
1.5384	0.4153	1.4969	0.5723	0.2429	1	0.3823	0.1623
1.3333	0.2	1.7091	0.7825	0.3608	1	0.4579	0.2111
	0.4	1.3014	0.4947	0.2067	1	0.3801	0.1588
1	0.2	1.2425	0.5625	0.2519	1	0.4527	0.2027
	0.4	0.9589	0.3549	0.1496	1	0.3701	0.1560
	0.415	0.9427	0.3427	0.1414	1	0.3635	0.1500

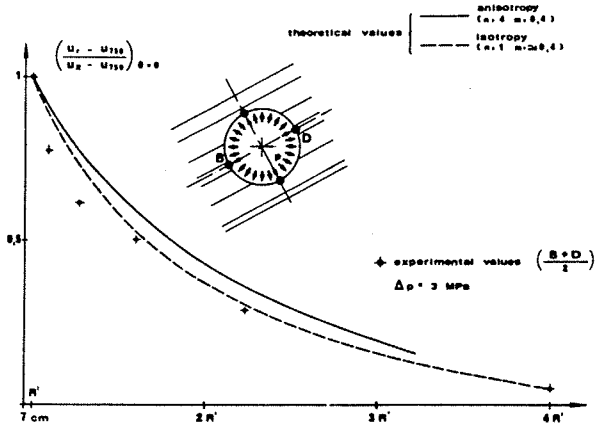

FIG. 10 Comparison between experimental and theoretical values (ratios) of radial displacements along the diameter parallel to the stratification.

We can interpret the measurements for Δp = 3 MPa referring to the points at 7 cm depth ($u_{R'}$, for R' = 157 cm).

We acknowledge (Table IV) an average radial displacement perpendicular to the stratification (A+C)/2 = (220+295)/2 = 257 μm and parallel to the stratification (B+D)/2 = (188+208)/2 = 198 μm.

The ratio between these displacements gives 257/198 = 1.30.

We now compare that value with the ratios between the relative displacements (in the two perpendicular directions) of Table VII.

For m = 0.4 we obtain by interpolation n $\simeq$ 1.43.

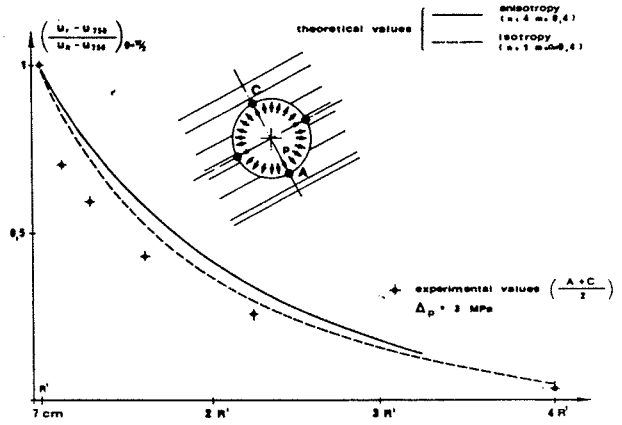

FIG. 11 Comparison between experimental and theoretical values (ratios) of radial displacements along the diameter normal to the stratification.

TABLE VII

$n = \frac{E_1}{E_2}$	$m = \frac{G_2}{E_2}$	$\frac{(u_{R'} - u_{750})\ \theta = \pi/2}{(u_{R'} - u_{750})\ \theta = 0}$
4	0.2	2.403
	0.4	2.340
	0.6	2.324
2.6666	0.2	1.929
	0.4	1.924
	0.6	1.934
2	0.2	1.603
	0.25	1.609
	0.3	1.562
	0.4	1.609
1.5384	0.4153	1.356
1.3333	0.2	1.230
	0.4	1.236
1	0.2	1
	0.4	1
	0.415	1

Always by interpolations, in Table V we find a value

$$\frac{(u_{R'} - u_{750})\ \theta = 0}{\Delta p \frac{R}{E_1}} \simeq 1.08$$

and therefore:

$$E_1 = \frac{1.08 \times \Delta p \times R}{(u_{R'} - u_{750})_{\theta=0}} = \frac{1.08 \times 3 \times 150}{0.0198} = 24545 \text{ MPa}$$

$$E_2 = \frac{E_1}{n} = 17165 \text{ MPa}$$

$$G_2 = m\, E_2 = 6866 \text{ MPa} \quad (m = 0.4)$$

5. RECENT IMPROVEMENTS OF HYDRAULIC PRESSURE CHAMBER TESTING TECHNIQUE

The testing technique recently set up by ISMES has been successfully experimented in this investigation. This technique makes it possible to simplify the problem of load application to the rock surface (Fig. 12).

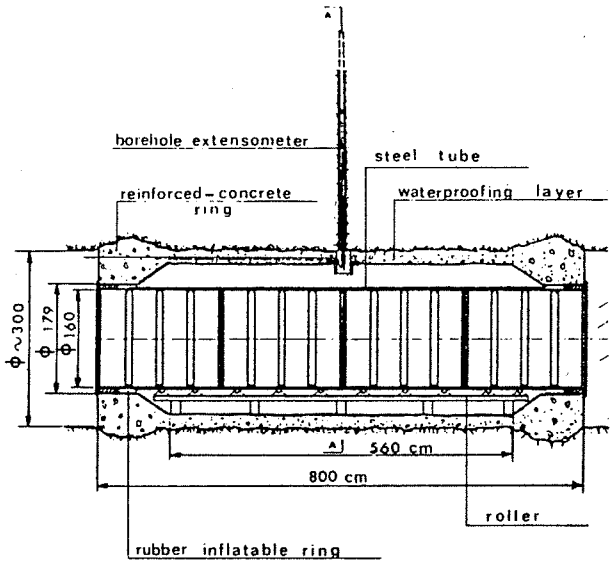

FIG. 12 Scheme of hydraulic chamber showing loading and measuring equipment.

Previous procedure planned the closing of the experimental tunnel by two reinforced concrete plugs and the casting of a concrete lining on the lateral surface of the tunnel. Groutings at subsequent stages ensured the bonding between the concrete lining and the underlying rock. The construction of these expensive works did not allow a frequent use of the hydraulic chamber; therefore, an effort was made to simplify the testing technique.

Now, only two concrete rings at the ends of the chamber are built and the lining of the tunnel lateral surface is realized by a layer of 5 to 10 cm thick spritz-beton, over which a waterproofing lining made with PVC sheets is applied (Fig. 13). The use of spritz-beton considerably reduces the preparation time of pressure application surfaces, making it possible also to exclude the grouting which, by using the previous technique, was necessary to ensure the bond between the concrete lining and the underlying rock. A large-diam central pipe (Ø = 1600 mm), made of composite elements and standing on a base roller, supports the hydrostatic pressure, while the water sealing is ensured by two inflatable rubber rings, inserted between the steel pipe extrados surface and the end rings. The tunnel stretch which is generally involved in the test is 8 m long. Radial holes are bored at the median section; their depth is twice the tunnel diameter. Special multibase strain gauges inside the boreholes make it possible to measure the rock mass displacements at various depths from the loading surface.

The new technique, besides considerably reducing the testing time and costs up to 40%, compared with the

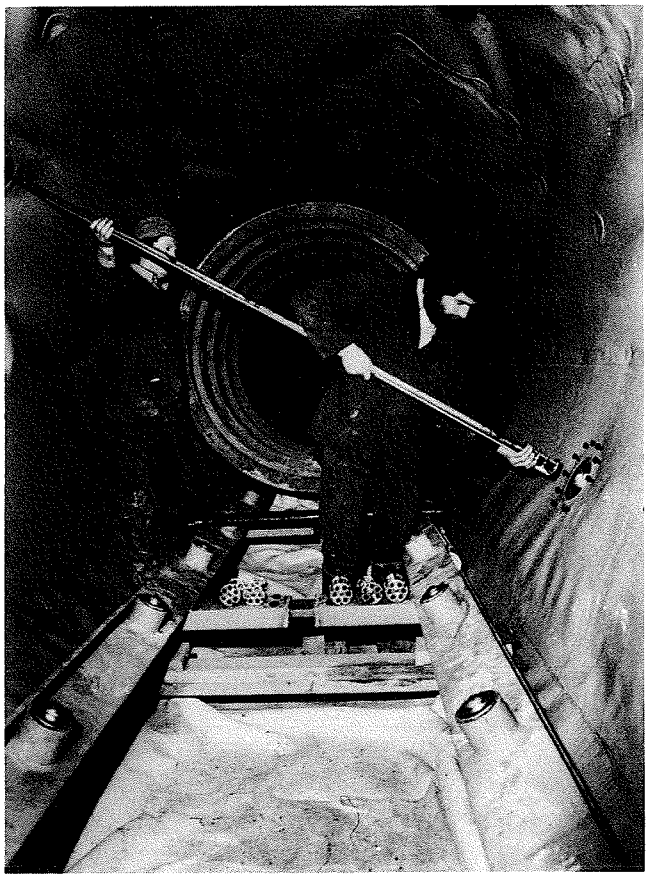

FIG. 13 The inside of hydraulic chamber during the installation of radial borehole extensometers

previous technique, presents additional non-negligible advantages, since it may be used with various-diam tunnels and does not stop the transit through the tunnel during the preparation and performance of the test.

ACKNOWLEDGEMENTS

The authors wish to thank Dr. R. Di Bacco of Mathematical Dept. of ISMES for the valuable collaboration.

REFERENCES

Borsetto, M., Goffi, L., Rossi, P.P. (1981)
Studio di ammassi rocciosi stratificati riferito a prove di deformabilità in cunicolo.ISMES Bull.no.151

Goffi, L. (1972)
La determinazione delle costanti elastiche di ammassi rocciosi ortotropi mediante prove in sito. L'Energia Elettrica no. 10

Goffi, L., Rossi, P.P., Borsetto, M. (1978)
Interpretazione di tecniche sperimentali per la misura dei parametri di deformabilità di ammassi rocciosi. Atti dell' Istituto di Tecnica delle Costruzioni del Politecnico di Torino, no. 112- ISMES Bull. no. 113

Lekhnitskii, S.G. (1963)
Theory of elasticity of an anistropic elastic body. Holden Day

Oberti, G., Carabelli, E., Goffi, L., Rossi, P.P. (1979)
Study of an orthotropic rock mass: experimental techniques, comparative analysis of results. Proceedings IV International Congress of ISRM, Montreux

Oberti, G., Goffi, L., Rebaudi, A. (1970)
Comportement statique des massifs rocheux (calcaires) dans la réalisation de grands ouvrages souterrains. Proceedings II International Congress of ISRM, Beograd

Pinto, J.L. (1966)
Stresses and strains in an anisotropic-orthotropic body. Proceedings of the I Congress of ISRM, Lisboa